

Remediation of Cr(VI) and Pb(II) Aqueous Solutions Using Supported, Nanoscale Zero-valent Iron

SHERMAN M. PONDER,[†]
JOHN G. DARAB,[‡] AND
THOMAS E. MALLOUK^{*†}

Department of Chemistry, The Pennsylvania State University,
State College, Pennsylvania 16803, and Pacific Northwest
National Laboratory, Richland Washington 99352

Borohydride reduction of an aqueous iron salt in the presence of a support material gives supported zero-valent iron nanoparticles that are 10–30 nm in diameter. The material is stable in air once it has dried and contains 22.6% iron by weight. The supported zero-valent iron nanoparticles ("Ferragels") rapidly separate and immobilize Cr(VI) and Pb(II) from aqueous solution, reducing the chromium to Cr(III) and the Pb to Pb(0) while oxidizing the Fe to goethite (α -FeOOH). The kinetics of the reduction reactions are complex and include an adsorption phase. About 10% of the iron in the material appears to be located at active surface sites. Once these sites have been saturated, the reduction process continues but at a much lower rate, which is likely limited by mass transfer. Rates of remediation of Cr(VI) and Pb(II) are up to 30 times higher for Ferragels than for iron filings or iron powder on a (Fe) molar basis. Over 2 months, reduction of Cr(VI) was 4.8 times greater for Ferragels than for an equal weight of commercial iron filings (21 times greater on the basis of moles of iron present). The higher rates of reaction, and greater number of moles of contaminant reduced overall, suggest that Ferragels may be a suitable material for in situ remediation.

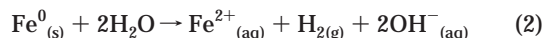
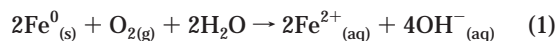
Introduction

Inorganic contamination is a significant environmental hazard to drinking water supplies. The U.S. EPA action level for chromium is 0.1 mg/L for Cr, while for Pb it is 0.015 mg/L (1, 2). Additionally, the EPA has set a Maximum Contaminant Level Goal for Pb of 0 mg/L (3). Most of the contamination comes from steel mill runoff and erosion of natural deposits in the case of Cr and from corrosion of household plumbing and natural erosion in the case of Pb (4). The EPA estimates that as many as 40 million U.S. residents may use water with Pb levels higher than the action level of 0.015 mg/L.

The use of zero-valent iron for in situ remediation has expanded to include several kinds of reducible contaminants. Much of this research originally focused on the remediation of chlorinated hydrocarbons in aqueous streams (5–11). More recently, remediation by zero-valent iron has been applied to other contaminants (12–15). While several studies have examined the reduction of Cr(VI) by zero-valent iron

(12, 16, 17), very little work has been performed on the reduction of aqueous Pb(II) (18, 19).

Zero-valent iron removes aqueous contaminants by reductive dechlorination, in the case of chlorinated solvents, or by reduction to an insoluble form, in the case of aqueous metal ions. Iron also undergoes redox reactions with dissolved oxygen and water.



One important parameter in the rate at which remediation of all these analytes occurs is the surface area of the zero-valent iron particles. It follows that increasing the surface area of the iron should also increase the rate of remediation. Previous work using nanoscale zero-valent iron formed by borohydride reduction suggested that the kinetics follow the general equation

$$v = kA_s [\text{Me}] \quad (3)$$

in which v is the rate, k is the rate constant ($\text{M}^{-1} \text{m}^2 \text{s}^{-1}$), Me is the metal contaminant (M), and A_s is the surface area of the iron particles (m^2) (20). However, this equation may not be universally applicable because it makes the following assumptions: (1) that reactive surface sites of the iron are far below saturation, (2) that the rate constant does not depend on initial metal ion concentration, and (3) that the reaction is monophasic and first order. Other studies in the literature on reduction of organics by iron filings have shown that reduction rates depend not only on the initial iron concentration but also on the initial concentration of contaminant (6, 9, 21, 22). Also, there appears to be an initial phase of the reaction in which the contaminant is sorbed onto the iron at a faster rate than it is reduced (10, 22). These complicating factors suggest that the overall kinetics cannot be simple first order, and other more complicated mixed-order models have been proposed (21–23).

In this study, nanoscale particles of zero-valent iron, 10–30 nm in diameter, were prepared by borohydride reduction of an aqueous iron salt (24). The reduction is done in the presence of a support material, which may be a polymeric resin, silica gel, or sand, and the product is a solid black material in which nano-iron is bound to the support. The use of a support prevents agglomeration of the iron and therefore presents a higher specific surface area of iron to the aqueous stream. The use of a support for nanoscale metal particles is a common practice for heterogeneous catalysis for a similar reason (25).

In this study, supported zero-valent iron particles formed by borohydride reduction ("Ferragel") were tested for their ability to separate and immobilize Cr(VI) and Pb(II) ions from aqueous solution. Comparisons were made between commercial iron powder and iron filings, unsupported nanoscale iron, and nanoscale iron supported on a commercial polymer resin.

Experimental Section

Synthesis of Materials. In a typical Ferragel synthesis, 10.00 g of $\text{FeSO}_4 \cdot 7\text{H}_2\text{O}$ was dissolved in 100 mL of 30% technical grade ethanol, 70% deionized water (v/v). Support material (4.00 g) was added while stirring. The pH was adjusted to about 6.8 with 3.8 M NaOH. NaBH_4 powder (1.8 g) was added incrementally to the mixture, allowing the foaming to subside

* Corresponding author phone: (814)863-9637; fax: (814)863-8403; e-mail: tom@chem.psu.edu.

[†] The Pennsylvania State University.

[‡] Pacific Northwest National Laboratory.

between increments. After addition of all of the NaBH_4 , the mixture was stirred for 20 min and then filtered through a $0.2 \mu\text{m}$ filter. Just prior to formation of a liquid meniscus between the solid particles, the solid was washed twice with technical grade ethanol, effectively substituting ethanol for the water in the mixture. This step helps to prevent immediate rusting as the filtration process is completed. The resulting black solid was vacuum-dried overnight and then broken up with a spatula to form a fine black powder.

While this preparation method was satisfactory at this scale, larger batches (100 g or more) showed significant rusting in the finished product, suggesting that a faster method of drying is needed for large scale production. Alternatively, the reaction could be done in an inert atmosphere, but the caveat here is that introduction of oxygen to nonpassivated zero-valent iron causes a strongly exothermic redox reaction. Atmospheric oxygen must be reintroduced slowly to the vacuum in order to allow the generated heat of this reaction to dissipate. Otherwise, the high surface area supported iron may ignite spontaneously.

Iron-on-resin Ferragels were made using mixed grade (20–30 μm) PolyFlo resin as the support. PolyFlo is a nonporous, hydrophobic resin available from PureSyn, Inc., Malvern, PA. This resin was chosen as a support because it is unreactive with borohydride and aqueous metal ions, and because it provides a high surface area upon which to disperse the nano-iron.

Iron filings (~40 mesh, Fisher) were used as received. Iron powder (–325 mesh, J. T. Baker) and electrolytically pure iron chunks (10–30 mesh, 99.999%, Aldrich) were also used as received. It has been noted that an HCl wash can improve the activity of these commercial materials, but because this step is unlikely to be implemented in real applications, it was not used in this work. Therefore all comparisons of rates are derived from as-received iron materials. To gauge the influence of borohydride on the iron activity, “activated” iron filings were prepared by substituting an equimolar amount of iron powder (Baker) for the iron salt, omitting the support, and using the same procedure for Ferragel synthesis. To assay the effect of the support itself on contaminant removal, treated resin was prepared by omitting the iron salt in the same procedure.

Batch Tests. Typically, Ferragel was tested by adding the solid directly to 100 mL of metal ion solution in a 125 mL high density poly(ethylene), HDPE, bottle. The pH was measured but not actively controlled, and no added buffers were used in these experiments. For Cr(VI), CrO_3 (Aldrich) was used as received, while $\text{Pb}(\text{C}_2\text{H}_3\text{O}_2)_2$ (Aldrich) was used (as received) for Pb(II). Rate constants were measured by adding 0.100 g of material to 100 mL of a 0.500 mM solution of the metal contaminant. At timed intervals, samples were taken by needleless, HDPE, 3 cm^3 syringe, filtered through a $0.2 \mu\text{m}$ poly(vinylidene fluoride), PVDF, syringe filter (Acrodisc), and tested for metal ion content using a Perkin-Elmer Model 530 Atomic Absorption spectrometer (AAS). Each bottle was given four sharp shakes every 2 min during the first 10 min of exposure, then every 5 min thereafter. This mixing method was used to help avoid the incidental passage of solids through the syringe filter and to prevent clumping caused by magnetic stirring. Control experiments to test variation of mass transfer rates against this method used a shaker table for mixing but showed no difference ($\pm 0.4 \mu\text{mol}$) in either the reduction rate of the contaminant or the iron content.

To test the relative reduction rates of iron filings, unsupported nano-iron, and Ferragel over the longer term, an amount of each material containing 1.414 mmol of iron (0.100 g of filings, 0.239 g of nano-iron, 0.465 g of Ferragel) was mixed with 1.000 L of 1.500 mM CrO_3 and 1.000 L of 1.500

TABLE 1. Comparison of Rates for Various Forms of Zero-valent Iron

type of iron	mmol Fe/g	apparent rate constant for	
		Cr(VI) (h^{-1})	Pb(II) (h^{-1})
resin-supported Ferragel	4.05	1.18	1.44
iron filings, ~40 mesh	14.1	0.22	0.09
iron powder, –325 mesh	14	0.24	0.05
“activated” iron powder, –325 mesh		0.28	0.33
high purity iron chunks, 10–30 mesh	18	0.22	0.08
unsupported nano-iron	5.96	1.16	

mM $\text{Pb}(\text{NO}_3)_2$. No buffers were added to the solutions, and the initial pH was 2.67 for the Cr solution and 2.92 for the Pb. Samples were then taken over a period of 60 days.

Measurements. Iron content was determined using acid dissolution followed by AAS. X-ray powder diffraction (XRD) was performed using a Phillips XPert MPD diffractometer. X-ray photoelectron spectroscopy (XPS) was performed on a Kratos XSAM800 pci. Nitrogen BET surface analysis was performed using a Micromeritics ASAP 2010.

Results and Discussion

Material Characterization. The iron-on-resin Ferragels resulting from the borohydride reduction process contained 22.6% iron by weight, as determined by AAS. The surface area of the material was $24.4 \pm 1.5 \text{ m}^2/\text{g}$, with little or no hysteresis in nitrogen BET analysis. The surface area, by nitrogen BET, of the nonporous resin itself, after treatment with borohydride (but in the absence of iron) was 3–3.5 m^2/g , depending on the average diameter of the particles. The surface area of unsupported nano-iron, made in the absence of a support material, was $21.7 \pm 1.5 \text{ m}^2/\text{g}$. One can conclude from these results that the surface area of Ferragel derives primarily from the supported iron nanoparticles.

Remediation of Cr(VI) and Pb(II). The rates of removal and immobilization of aqueous Cr(VI) and Pb(II) could be fit to pseudo-first-order reaction kinetics in both the aqueous ion and the iron (Figure 1). For 100 mL of 0.50 mM metal solution and 0.100 g of Ferragel, the initial rates were 1.18 and 1.44 h^{-1} , respectively. By comparison, the initial rates for 0.100 g of commercial iron filings (~40 mesh, Fisher) were slower, 0.22 h^{-1} for Cr(VI) and 0.44 h^{-1} for Pb(II), even though there was 3.5 times as much iron in the filings as in the Ferragel. Other forms of zero-valent iron were also tested and were also substantially slower reductants (Table 1). Note that all commercial materials were used as received and contain differing amounts of iron due to carbonaceous inclusions.

From Figure 1, it is apparent that there is an initial sorption phase during which the rate of disappearance of the contaminant from solution is significantly faster than at later times. With Cr(VI) and Pb(II), this initial phase appears to be complete after 10 min, resulting in a flattening of the first-order kinetic plots. Thus, the overall mechanism is more complicated than suggested by eq 3. The fact that this initial high rate of removal, and the subsequent slowing of the rate, occurs regardless of contaminant species or concentration suggests that the mechanism is physical (i.e., that it involves occlusion of the zero-valent iron) rather than chemical.

XPS and XRD analysis show that Cr(VI) is reduced to Cr(III), while Pb(II) is reduced to Pb(0) and possibly other insoluble phases. Research on zero-valent iron and the reduction of chromium shows that the typical result from this redox reaction is a chromite, with some of the iron substituted for the chromium (17, 26). Based on these earlier

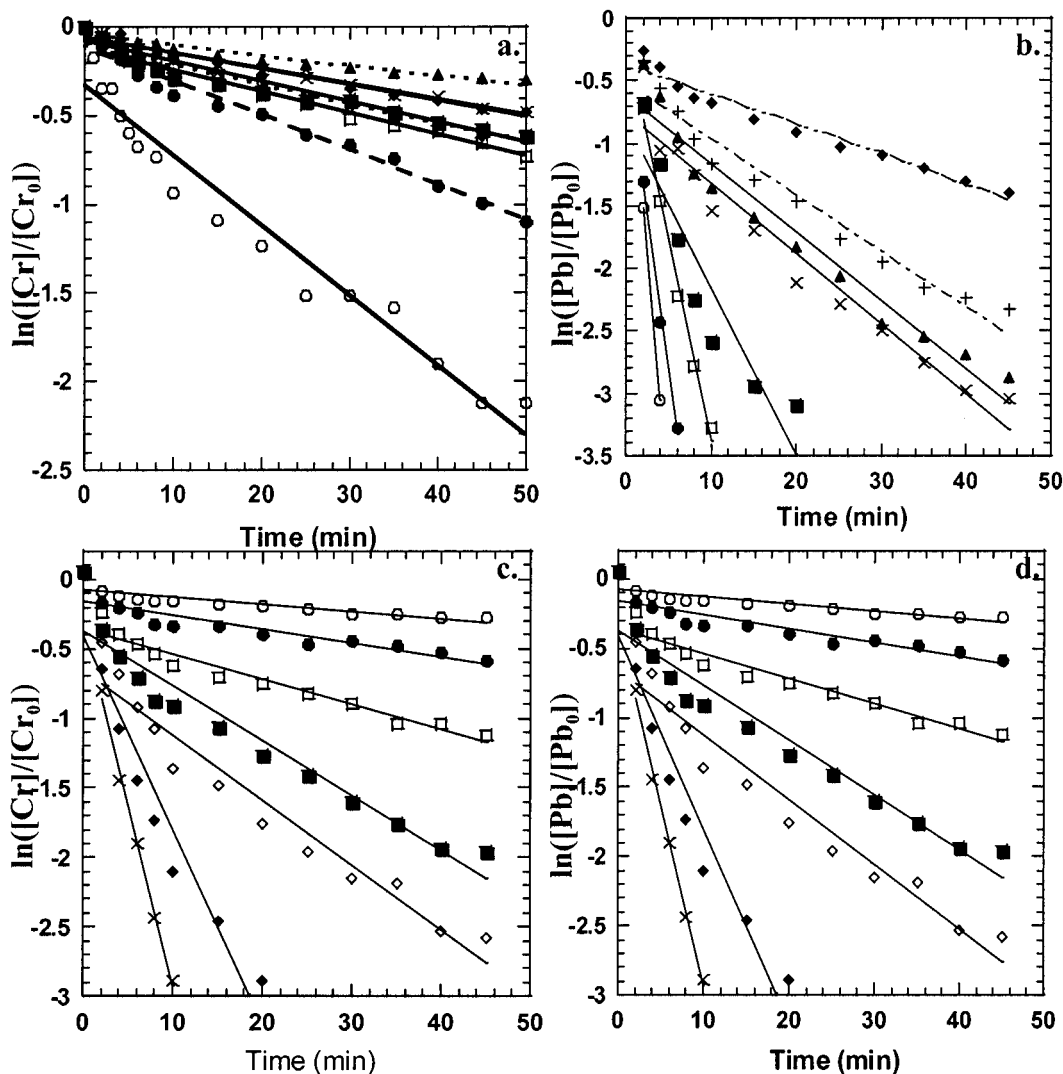


FIGURE 1. Comparison of first-order kinetics for reduction of Cr(VI) and Pb(II). a.: Cr(VI) reduction: 100 mL of Cr(VI) solution, 0.100 g of iron-on-resin Ferragel $\circ = 0.25$ mM, $\bullet = 0.50$ mM, $\square = 0.55$ mM, $\blacksquare = 0.65$ mM, $\diamond = 0.75$ mM, $\times = 0.85$ mM, and $\blacktriangle = 1.00$ mM. b.: Pb(II) reduction: 100 mL of Pb(II) solution, 0.100 g of iron-on-resin Ferragel. $\circ = 0.099$ mM, $\bullet = 0.149$ mM, $\square = 0.20$ mM, $\blacksquare = 0.25$ mM, $\times = 0.30$ mM, $\blacktriangle = 0.35$ mM, $+$ = 0.40 mM, and $\blacklozenge = 0.50$ mM. c.: Cr(VI) reduction: 100 mL of 0.50 mM Cr(VI) solution, iron-on-resin Ferragel solid. $\times = 0.190$ g, $\blacklozenge = 0.160$ g, $\diamond = 0.130$ g, $\blacksquare = 0.120$ g, $\square = 0.100$ g, $\bullet = 0.75$ g, $\circ = 0.50$ g. d.: Pb(II) reduction: 100 mL of 0.50 mM Pb(II) solution, iron-on-resin Ferragel solid. $\times = 0.175$ g, $\blacklozenge = 0.150$ g, $\diamond = 0.125$ g, $\blacksquare = 0.100$ g, $\square = 0.075$ g, $\bullet = 0.051$ g, $\circ = 0.029$ g.

studies, the chromium endproduct here is expected to have the same general chemical formula $(Cr_{1-x}Fe_x)(OH)_{3(s)}$, where x is typically about 0.33.

No previous data exist for Pb(II). To maximize Pb deposition, 0.5 g of Ferragel was exposed to 200 mL of 50 mM $Pb(C_2H_3O_2)_2$ for 30 days. XPS analysis of the resulting solid gave a surface composition of 8.2 atomic % Pb, 7.2 atomic % Fe, and 31.9 atomic % O with an approximate sampling depth of 25 Å. At this depth, all of the Pb appeared to be in the 2+ oxidation state, with a peak at 138.7 eV, while the iron was oxidized to the 3+ state with a peak at 711.2 eV. Oxygen showed a binding energy of 531.7 eV (Figure 2). It is unclear whether the presence of surface Pb^{2+} is due to a passivation layer formed in the original solution, sorption of Pb^{2+} onto the surface from the solution, or air oxidation of Pb^0 formed in the reaction. The powder XRD patterns were complicated by the presence of iron oxides and oxyhydroxides but showed a progression of peaks consistent with Pb^0 . Diffraction peaks were also assigned to $Pb(OH)_2$ and $PbO \cdot xH_2O$; however, there were also strong lines in the pattern that could not be indexed (Figure 3). Pb has a substantial initial deposition overpotential (27) and therefore tends to

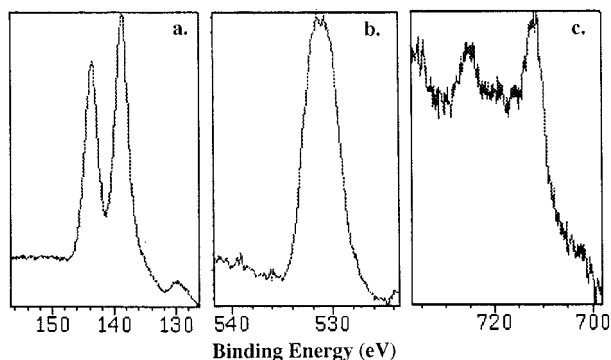


FIGURE 2. XPS of solids from 0.500 g Ferragel in 200 mL of 50 mM Pb(II) solution for 30 days. Graphitic carbon peak set at 284.6 eV. a: Pb peak at 138.7 eV. b: O peak at 531.7 eV. c: Fe peak at 711.2 eV.

grow in dendritic fashion. The high surface area of these deposits may favor adsorption of Pb^{2+} or air oxidation of zero-valent Pb species on these materials.

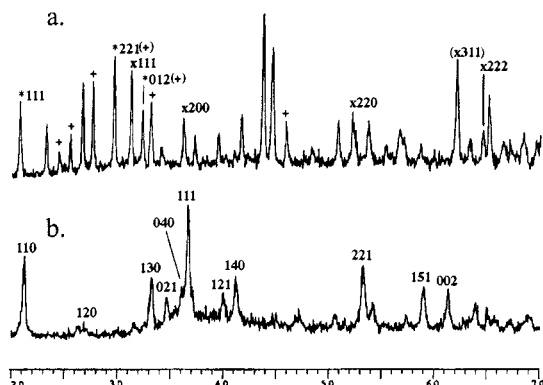
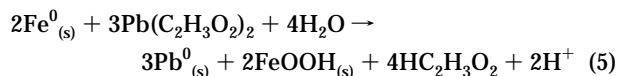
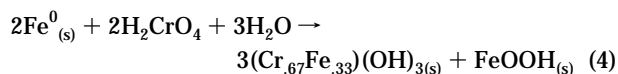


FIGURE 3. Powder XRD patterns and Miller indices of spent Ferragels. a: After exposure to Pb(II) solution. x = Pb(0), * = PbO·xH₂O (tentative), and + = Pb(OH)₂ (tentative, no indexing available). b: After exposure to Cr(VI) solution. Indexed peaks are for goethite (α-FeOOH).

The general reactions for the remediation of Cr(VI) and Pb(II) are thought to be



However, it is clear that one or more additional processes are in play in the Pb reaction and result in the formation of oxidized surface species.

Overall, 1.00 g Ferragel (4.05 mmol Fe) removed and immobilized 0.12 mmol of Cr(VI), or 0.18 mmol of Pb(II), from solution, based on tests of 0.5 g in contact with 100 mL of 50 mM solutions for 8 days. Under the same conditions, iron filings removed less than 0.01 mmol of Cr(VI) from solution. Over 68 days, Ferragel removed 0.625 mmol of Cr, giving an average removal rate of 0.0185 mmol Cr/day/g material (4.56 mmol/day/mol Fe). In contrast, iron filings removed 0.13 ± 0.03 mmol Cr in 102 days, with an average removal rate of 0.0026 mmol Cr/day/g material (0.147 mmol Cr/day/mol Fe). The Ferragel rate of removal was 7.1 times that of the iron filings, on a material weight basis, and 31 times faster than iron filings on a (Fe) molar basis. In terms of total amounts, Ferragel removed 4.8 times more Cr(VI) than an equal weight of iron filings and 21 times more Cr(VI) than an equal number of moles of iron filings.

As a control experiment, 0.100 g of borohydride-treated PolyFlo was also tested. This amount of support material adsorbed minimal amounts of contaminants (0.003 mmol Cr(VI) over 74 days and 0.020 mmol of Pb(II) over 7 days), demonstrating that nano-iron is the active ingredient in the Ferragel. PolyFlo is hydrophobic, and addition of larger amounts of resin to the container (125 mL of HDPE) causes agglomeration and does not increase total sorption. Interestingly, the resin-supported Ferragels are hydrophilic and are completely wetted by aqueous solutions.

As expected from eq 3, the apparent rate constant (k^*A_s) increases linearly with the amount of iron used. However, the apparent rate constant decreases with increasing initial concentrations of metal contaminant (Figure 4). A similar rate dependence on initial concentration has been noticed by other researchers in the reduction of CCl₄, chlorinated ethenes, and nitroaromatics (9, 21, 22, 28). That this rate dependence also occurs with aqueous inorganics suggests that it is a consequence of the oxidation kinetics of zero-valent iron and is not a specific effect of the analyte being reduced. This supports the notion that kinetic equations

worked out for other contaminants should be directly applicable to other systems that use zero-valent iron as the reductant (21–23). Indeed, this generalized applicability was the stated intent of Gotpagar et al. (23). While the apparent rate constant is expected to increase monotonically as the iron content (and therefore, the total iron surface area, A_s) is increased, the rate dependence on initial metal concentration demonstrates that eq 3 is inadequate to describe the kinetic behavior of the system.

There is a dramatic increase in the apparent rate constant when the number of moles of iron used is more than about 10 times the number of moles of contaminant. The increase in apparent rate constant is 10 times larger in the case of Pb(II) and about five times larger in the case of Cr(VI). This consistent breakpoint in the apparent rate constants suggests that only 8–10% of the iron in Ferragels is present at active surface sites. At iron contents below the breakpoints, these surface sites are saturated, and mass transfer of the analyte to the occluded zero-valent iron becomes rate-limiting. The breakpoints are presented as a percentage of total iron but cannot easily be translated into a number of active surface sites. To do this, a quantitative assessment of the surface morphology, mass transfer, and sorption kinetics, and ultimately the rate constant of the reaction, would be needed (29). It should also be noted that complex kinetics should make linear kinetic fits (such as those shown in Figure 4) inaccurate. It may be that the range of concentrations used in these experiments simply fell within the pseudo-first-order regime of an overall combined-order kinetic system.

In longer term (60 day) experiments, unsupported nano-iron outperformed Ferragel in remediating Cr, but Ferragel reduced significantly more Pb (Figure 5). Both forms of nano-iron far outperformed iron filings (Fisher). It is also interesting that 90% of the total removal of contaminant occurred within the first 48 h, suggesting that even in column or in situ barriers the primary reduction process occurs upon first contact of iron with the analyte. The pH after 60 days in the Cr solution was 3.25 with Ferragel, 2.99 with unsupported nano-iron, and 2.71 with iron filings. For the Pb solutions, the final pH was 4.01 with Ferragel, 3.62 with nano-iron, and 3.12 with iron filings. The Fe content of the solution in all cases was below the detection limit of 1.8 μM.

The reason for the additional reduction of Cr by unsupported nano-iron, which began after the first 24 h and ended with about 5% (0.075 mmol Cr) more reduced than with Ferragel, is unknown at this time. As expected, the initial rates for similarly sized iron nanoparticles, when normalized to the number of moles of iron present, are very nearly equal (Figure 6). Likewise, the substantially more efficient removal of Pb (35%, 0.525 mmol Pb) from solution by Ferragel compared to unsupported nano-iron is surprising since the number of moles of iron used were equal. Given that the total surface area of the supported nano-iron is only slightly higher than that of unsupported nano-iron, a 35% increase in total remediation is unexpected. As a blank, 0.100 g of borohydride-treated resin was mixed in 100 mL of 0.500 mM Pb solution for 7 days but removed only 0.200 mmol of aqueous Pb/g of PolyFlo. For the above experiment, resin content is estimated at 0.36 g of the Ferragel, and Pb removal due to the resin is estimated at 0.072 mmol. These results are under further investigation.

Applicability to in Situ Remediation. There are three important factors that determine the utility of a zero-valent iron material for in situ remediation. One is the iron content, since the amount of iron must at least be sufficient to react stoichiometrically with the contaminant. For most contaminated plumes, the overall concentration is low, in the ppm or ppb range. However, because of the slow flow of groundwater and the partitioning of contaminants in to and out of the solid phase, a typical plume may require 100–200 years to travel past a given point. The second factor is how efficiently

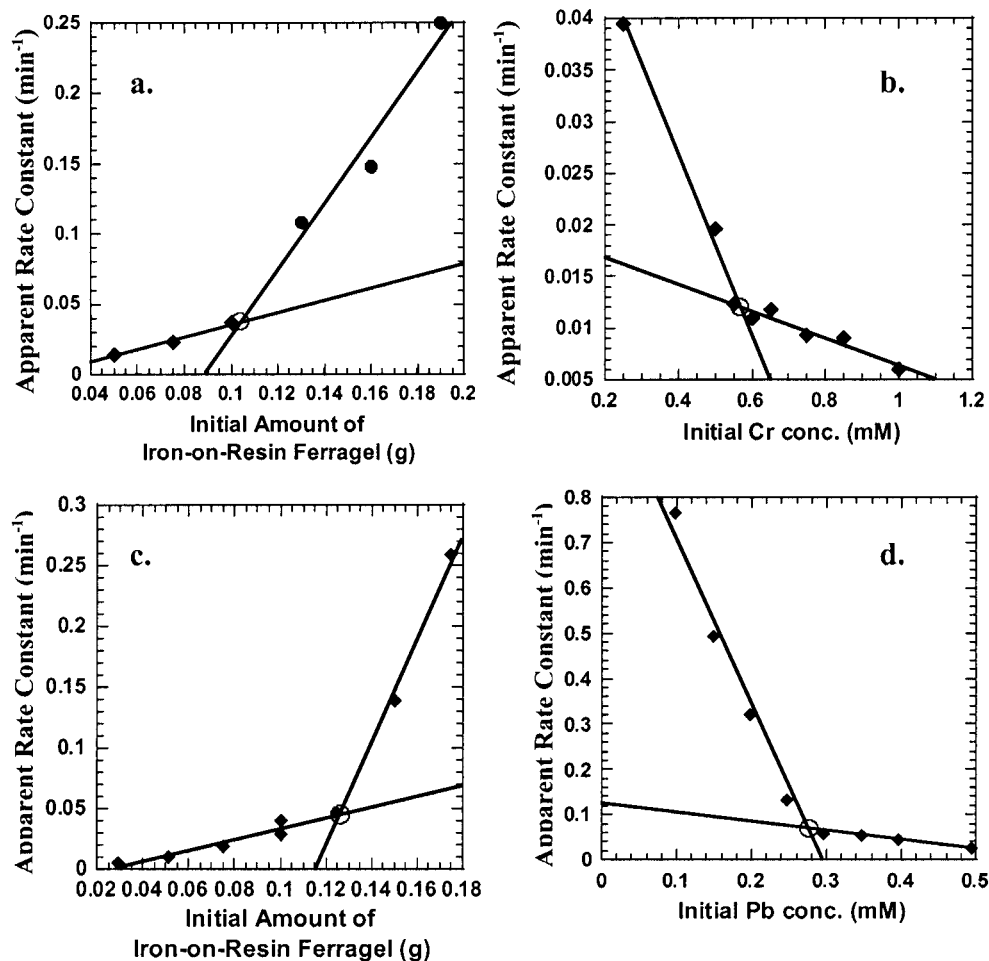


FIGURE 4. Breakpoints of apparent rate constants for iron-on-resin Ferragel. a: 100 mL of 0.50 mM Cr, ○ = 0.104 g solids (0.42 mmol Fe). b: 0.100 g solids (0.405 mmol Fe) in 100 mL of Cr solution, ○ = 0.57 mM Cr. c: 100 mL of 0.50 mM Pb, ○ = 0.126 g solids (0.510 mmol Fe). d: 0.100 g solids (0.405 mmol Fe) in 100 mL of Pb solution, ○ = 0.278 mM Pb.

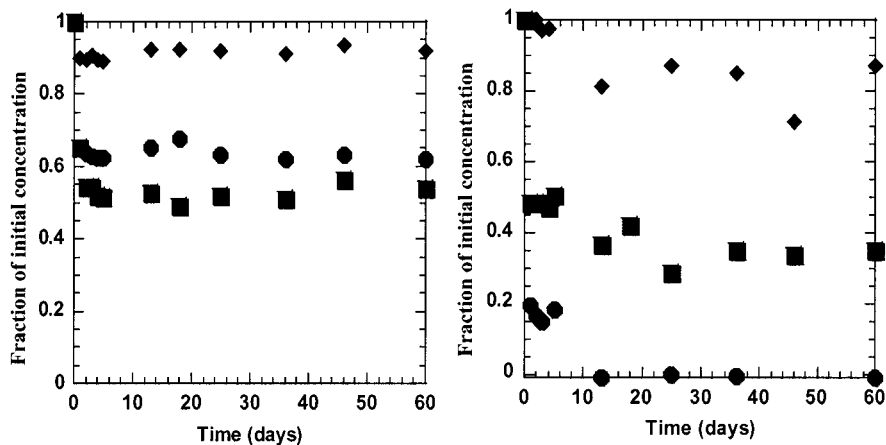


FIGURE 5. Fractions of initial concentrations remaining for 1.000 L of 1.500 mM solutions after exposure to zero-valent iron materials containing 1.414 mmol Fe. a: Cr(VI). b: Pb(II). Circles are 0.465 g of iron-on-resin Ferragel, squares are 0.239 g of unsupported nano-iron, and diamonds are 0.100 g of iron filings (Fisher).

the reductant is used. Excavation is the most costly capital expense in in situ remediation. The ability to reduce a greater number of moles of contaminant for the same number of moles of iron means that it is likely that a smaller volume of barrier material is needed for a specific application, and thus, the total excavation volume can be reduced. The third factor is the corrosion rate of the iron, which must be considered because reactions 1 and 2 are thermodynamically favorable. It is important that these reactions be sufficiently slow in the time scale of the remediation process.

In terms of reduction rates for Cr, zero-valent iron nanoparticles are 7–12 times faster than equivalent weight of iron powder. When the data are normalized to the number of moles of iron in each material (Figure 6), the rate of reduction is 30 times faster for iron nanoparticles. The total amount of Cr(VI) removed over 60 days from a 1.500 mM solution was 4.8 times more for Ferragel compared to an equimolar amount of iron filings. This means that iron nanoparticles, with their larger surface area, have a significantly higher atom efficiency for reductive remediation of

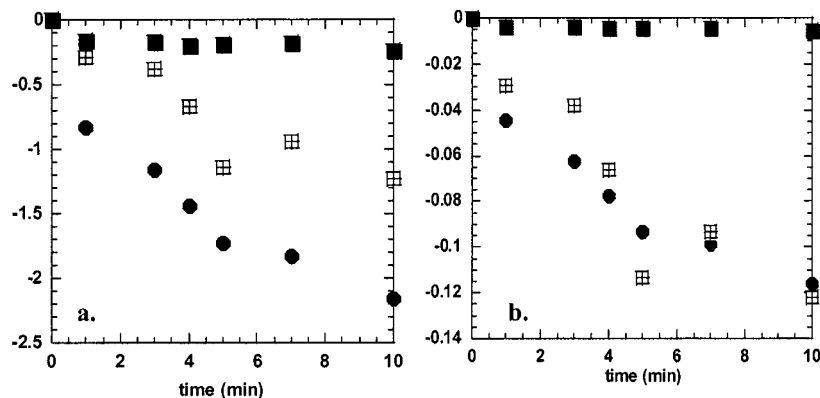


FIGURE 6. a: Removal of Cr(VI) from 100 mL of 0.50 mM solution by 0.100 g of supported nano-iron (Ferragel), unsupported nano-iron, and iron powder (-325 mesh, Baker). b: The same data normalized per mol of iron present shows equivalent rates for nano-iron with or without support. Both kinds of nano-iron far outperform the iron powder. Solid circle is unsupported nano-iron, crosshatched square is nano-iron on a resin support (Ferragel), and solid square is unsupported iron powder.

contaminants. Atom efficiency refers to the fraction of iron atoms that can be used in the reaction and is directly related to the accessibility of the iron. The combination of high reaction rates and higher atom efficiency suggests that Ferragels will allow for significantly smaller excavation volumes when used for in situ remediation of contaminated groundwater flows. However, the batch tests reported in this study do not provide for a constant influx of water and dissolved oxygen. Thus, the greater atom efficiency may not translate directly to column or field tests, and additional characterization (particularly of the corrosion rate under realistic conditions) is needed. Additionally, batch tests do not consider hydraulic conductivity. Clumping of nanoparticles would adversely affect permeability and would impede the flow of groundwater through an in situ barrier. Whether Ferragel particles would clump in situ, and whether this effect could be eliminated by using larger support particles or by pelletizing the Ferragel remains to be seen.

One issue that should be considered for practical applications is the presence of humic and fulvic acids in natural waters. These compounds could possibly ligate the iron, especially Fe(II), and alter the activity. This effect is unlikely to cause serious problems because of the low affinity of these acids to iron in neutral to alkaline waters (30). Recent work suggests that in acidic waters, natural organic material may be used to aid in the reduction of contaminants such as Cr(VI) (31).

A second issue to be investigated is the relative reactivity and atom efficiency of different forms of irons, when measured over long time periods that are relevant to remediation of slow-moving plumes. While Ferragels clearly make more efficient use of iron atoms in the short term, it remains to be seen if less active forms of zero-valent iron can attain high atom efficiencies over time periods of decades to hundreds of years. Accelerated tests of corrosion and reactivity are currently being conducted to estimate the relative performance of Ferragels and other forms of iron under these conditions.

Acknowledgments

This work was supported by the U.S. Department of Energy under contract DE-FG07-97ER14822. Pacific Northwest National Laboratory is operated for the U.S. Department of Energy by the Battelle Memorial Institute under contract DE-AC06-76RLO 1830. Electron microscopy and X-ray microanalysis were performed at the Electron Microscope Facility for the Life Sciences in the Biotechnology Institute at the Pennsylvania State University.

Literature Cited

- (1) *Code of Federal Regulations*, Section 141.52, Title 40, p 407.

- (2) *Code of Federal Regulations*, Section 141.80, Title 40, p 425.
- (3) *Fed. Regist.* **65** (8), 1976.
- (4) *EPA Fact Sheet*, 15-F-92010.
- (5) Gillham, R. W.; O'Hannesin, S. F. *Ground Water* **1994**, *32*, 958.
- (6) Matheson, L. J.; Tratnyek, P. G. *Environ. Sci. Technol.* **1994**, *28*, 2045.
- (7) Hardy, L. I.; Gillham, R. W. *Environ. Sci. Technol.* **1996**, *30*, 57.
- (8) Orth, W. S.; Gillham, R. W. *Environ. Sci. Technol.* **1996**, *30*, 66.
- (9) Johnson, T. L.; Scherer, M. M.; Tratnyek, P. G. *Environ. Sci. Technol.* **1996**, *30*, 2634.
- (10) Burris, D. R.; Campbell, T. J.; Manoranjan, V. S. *Environ. Sci. Technol.* **1995**, *29*, 2850.
- (11) Roberts, A. L.; Totten, L. A.; Arnold, W. A.; Burris, D. R.; Campbell, T. J. *Environ. Sci. Technol.* **1996**, *30*, 2654.
- (12) Boronina, T.; Klabunde, K. J.; Sergeev, G. *Environ. Sci. Technol.* **1995**, *29*, 1511.
- (13) Devlin, J. F.; Klausen, J.; Schwarzenbach, R. P. *Environ. Sci. Technol.* **1998**, *32*, 1941.
- (14) Hundal, L. S.; Singh, J.; Bier, E. L.; Shea, P. J.; Comfort, S. D.; Power, W. L. **1997**, *97*, 55.
- (15) Singh, J.; Comfort, S. D.; Shea, P. J. *Environ. Sci. Technol.* **1999**, *33*, 1488.
- (16) Powell, R. M.; Puls, R. W.; Hightower, S. K.; Sabatini, D. A. *Environ. Sci. Technol.* **1995**, *29*, 1913.
- (17) Blowes, D. W.; Ptacek, C. J.; Jambor, J. L. *Environ. Sci. Technol.* **1997**, *31*, 3348.
- (18) Blowes, D. W.; Ptacek, C. J.; Benner, S. G.; McRae, C. W. T.; Puls, R. W. *Groundwater Quality: Remediation and Protection*, IAHS Pub. no. 250; **1998**, 483.
- (19) Smith, E. H. *Water Res.* **1996**, *30*, 2424.
- (20) Wang, C.-B.; Zhang, W.-X. *Environ. Sci. Technol.* **1997**, *31*, 2154.
- (21) Johnson, T. L.; Fish, W.; Gorby, Y. A.; Tratnyek, P. G. *J. Contam. Hydrol.* **1998**, *29*, 379.
- (22) Wust, W. F.; Kober, R.; Schlicker, O.; Dahmke, A. *Environ. Sci. Technol.* **1999**, *33*, 4304.
- (23) Gotpagar, J. K.; Grulke, E. A.; Bhattacharyya, D. *J. Hazard. Mater.* **1998**, *62*, 243.
- (24) van Wontergem, J.; Morup, S.; Koch, C. J. W.; Charles, J. W.; Wells, S. *Nature* **1986**, *322*, 622.
- (25) *Encyclopedia of Chemical Technology*, 4th ed.; Kroschwitz, J., Howe-Grant, M., Eds.; J. Wiley & Sons: New York, 1993; Vol. 5, pp 340-348.
- (26) Pratt, A. R.; Blowes, D. W.; Ptacek, C. J. *Environ. Sci. Technol.* **1997**, *31*, 2492.
- (27) Kuhn, A. J. *The Electrochemistry of Lead*; Academic Press: New York, 1979.
- (28) Scheerer, M. M.; Tratnyek, P. G. *Natl. Meet., Am. Chem. Soc., Div. Environ. Chem., Abstr.* **1995**, *35*, 805.
- (29) Arnold, W. A. Ph.D. Thesis, The Johns Hopkins University, 1999.
- (30) Gu, B.; Schmitt, J.; Chen, Z.; Linag, Li; McCarthy, J. F. *Environ. Sci. Technol.* **1994**, *28*, 38.
- (31) Jardine, P. M.; Fendorf, S. E.; Mayes, M. A.; Larsen, I. L.; Brooks, S. C.; Bailey, W. B. *Environ. Sci. Technol.* **1999**, *33*, 2939.

Received for review October 5, 1999. Revised manuscript received March 6, 2000. Accepted March 29, 2000.

ES9911420